BET inhibitors synergize with anti-PD1 by rescuing TCF1^{+} progenitor exhausted CD8^{+} T cells in Acute Myeloid Leukemia

Kyle A. Romine[1], Hyun-jun Cho[2], Yoko Kosaka[2], Kaelan Byrd[2], Jesse L. Coy[2], Patrick A. Flynn[2], Matthew T. Newman[3], Christopher Loo[2], Jaime Scott[2] and Evan F. Lind[1,2,4]

[1]Department of Cell, Developmental & Cancer Biology, Oregon Health & Science University, Portland, OR, USA

[2]Department of Molecular Microbiology and Immunology. Oregon Health & Science University, Portland, OR, USA

[3]School of Medicine, Oregon Health & Science University, Portland, OR, USA

[4]Knight Cancer Institute, Oregon Health & Science University, Portland, OR, USA

Abstract

Many AML patients exhibit hallmarks of immune exhaustion such as increased myeloid derived suppressor cells (MDSCs), suppressive regulatory T cells (Tregs), and exhausted/dysfunctional T cells. Using a mouse model of AML driven by *FLT3-ITD and TET2* deficiency we found immune-related features in AML similar to patients, such as increased myeloid-derived suppressor cells (MDSCs) and regulatory T cells (Tregs). Moreover, we found that $CD8^+$ T cells derived from these mice exhibit a terminally exhausted phenotype (TEx $PD1^+$, $TIM3^+$, $TCF1^-$), which have been shown to be refractory to immune checkpoint blockade monotherapy. Here we show that small molecule drugs targeting BET proteins, in addition to targeting tumor-intrinsic factors, rescue T cell exhaustion and ICB resistance. *Ex vivo* treatment of cells from AML mice and primary AML patient samples with BET inhibitors (BETi) reversed $CD8^+$ T cell exhaustion by restoring proliferative capacity and expansion of more functional precursor exhausted T cells (TPEx; $PD1^+$, $TCF1^+$, $TIM3^-$). This reversal is enhanced by combined BETi and anti-PD1 treatment. Finally, we show that BETi synergizes with anti-PD1 *in vivo*, resulting in the reduction of circulating leukemia cells, enrichment of $CD8^+$ T cells in the bone marrow, and increased expression of *TCF7*, *SLAMF6,* and *CXCR5* in $CD8^+$ T cells. In total, by using a murine model, we show the potential efficacy of combining BETi and ICB therapy in the treatment of AML.

Introduction

Acute Myeloid Leukemia (AML) is a myeloid lineage cancer with a poor prognosis and with limited therapeutic options for those who cannot withstand current frontline therapies[1-3]. For other difficult-to-treat cancers, such as metastatic melanoma, therapy with immune checkpoint blockade (ICB) has filled this void for many patients and has made meaningful increases in life expectancy[4, 5]. ICB functions to reinvigorate cancer-specific T cells via blockade of inhibitory immune checkpoint (IC) receptors which suppress T cell activity and function. Expression of IC receptors, which include CTLA-4, PD1, TIM3, LAG3, TIGIT, VISTA, and others, increases after initial antigen exposure and regulates T cell function through various signaling pathways. It has been hypothesized that these receptors are an evolutionary adaptation to chronic antigen exposure to prevent the development of autoimmunity after infection. Recent work has identified unique subsets of $CD8^+$ T cells that are generated specifically during chronic antigen exposure. These T cell subsets are referred to as Terminally Exhausted T cells (TEx), which have high expression of inhibitor receptors such as TIM3, and progenitor exhausted T cells (TPEx), which have high expression of TCF1 and SLAMF6. TPEx have specifically been

shown to expand in response to anti-PD1 therapy and retain anti-tumor capacity[6-10]. In contrast, TEx are significantly more dysfunctional with a lack of proliferative capacity and dramatically reduced secretion of effector molecules, such as granzyme B and perforin[6-8, 11-14]. Our lab and others have recently shown that a proportion of blood and bone marrow specimens from AML patients have an immunosuppressive microenvironment and have hallmarks of immune exhaustion: increased frequency of Tregs[15] and MDSCs[16], decreased T-cell proliferation[17], elevated expression of immune checkpoint molecules[18-20] and increased TEx vs. TPEx[20, 21] populations. Importantly, a subset of these patient samples containing dysfunctional T cells can be rescued by immune checkpoint blockade[17]. This prompted us to further investigate potential combination treatment regimens by which we could reduce T cell exhaustion in AML.

The Bromodomain and Extra-Terminal domain (BET) protein family is made up of bromodomain-containing proteins BRD2, BRD3, BRD4, and BRDT[22-26]. BET proteins are epigenetic readers which bind acetylated histone residues via conserved BD1 and BD2 domains and mediate downstream functions, such as histone acetylation recognition, chromatin remodeling, and transcription regulation. BRD4 binds acetylated histone tails and recruits Positive Transcription Elongation Factor b (P-TEFb) to enhancer regions to mediate the phosphorylation of the c-terminal domain of RNA pol II, required for elongation of the nascent mRNA[23, 27]. RNAi screening studies identified BRD4 loss as a potent and selective inhibitor of leukemic growth and treatment with BETi induced leukemia cell death *in vitro* and *in vivo*[22, 25, 26, 28-31]. Clinically however, BETi therapy was able to elicit some complete remissions but ultimately failed as a monotherapy in the majority of patients[32]. Interestingly, BETi have also been shown to positively affect $CD8^+$ T cells, directly or indirectly, via reduction of PD-L1 expression on myeloid cells[33, 34] and inhibition of chronic TCR activation genes, such as BATF, which increased the persistence of stem-cell like memory $CD8^+$ T cells[35]. Therefore, we hypothesized that BETi may synergize with anti-PD1 therapy in AML through targeting of tumor-intrinsic factors, such as myc, and tumor-extrinsic factors, such as promoting T cell stemness. Accordingly, we show that a *FLT3-ITD/TET2* AML mouse model phenocopies the immune exhaustion and PD-1 refractoriness found in AML patients. We found that these mice have a dramatically increased ratio of TEx:TPEx compared to WTs and that BETi can rescue immune exhaustion by promoting proliferation of TPEx $CD8^+$ T cells. In addition, we found that BETi rescued T cell exhaustion in a subset of AML patient samples. Finally, BETi treatment was found to have a synergistic

effect with anti-PD1 *in vivo* and *ex vivo* by reducing leukemic tumor burden and increased RNA expression of TPEx gene programs while decreasing TEx gene programs.

Results

FLT3-ITD/TET2 Mice Exhibit hallmarks of immune exhaustion.

We previously showed that a genetically-engineered mouse model, *FLT3-ITD*$^{+/-}$ *TET2*$^{flox/+}$ *LysM-Cre*$^{+/-}$ displays a profound defect in T cell proliferative capacity[36]. To further characterize the tumor microenvironment and functional capacity of T cells derived from AML mice we performed multi-color flow cytometry to identify changes in myeloid and lymphoid populations, T cell exhaustion markers, and histology at multiple organ sites. Accordingly, we found dramatically increased levels of CD11b^{+} myeloid cells in the spleens and blood of AML mice compared to WT C57BL/6 mice (Fig 1a, b). In addition, we found significant evidence of myeloid tumor infiltration in the spleen—causing splenic follicle disruption and infiltration in liver portal veins and bone marrow (Fig 1c). Furthermore, we found increased levels of GR1^{+} myeloid-derived suppressor cells (MDSCs) and CD4^{+}FOXP3^{+} regulatory T cells (Tregs), a frequent occurrence in AML patients[15-17, 19, 37](Fig S1a, b), but no difference in T cell frequency (Fig S1c). Characterization of the lymphoid populations identified significant increases in multiple exhaustion markers in both the CD4^{+} and CD8^{+} T cell populations but most notably a significant decrease in T cell stem-like maintenance transcription factor TCF1 (Fig 1d,e). Taken together we concluded that the AML mice replicated the tumor microenvironment characterized by a terminal exhaustion T cell phenotype.

T cells derived from AML mice are dysfunctional and are phenotypically and show intrinsic functional exhaustion.

We previously showed that T cells from the AML mice are dysfunctional and unresponsive to TCR stimulation [36]. We assessed the proliferative potential of CD4^{+} and CD8^{+} T cells derived from AML or WT mice by plating CFSE-labeled splenocytes with anti-CD3 coated plates, thus relying on naturally occurring antigen-presenting cells for co-stimulation, and analyzed by flow cytometry. As shown previously, both CD4^{+} and CD8^{+} T cells derived from AML mice exhibited significantly reduced proliferation compared to WT mice in response to TCR stimulation (Fig 2a, b). We next asked whether the T cells were intrinsically dysfunctional or if the effect on proliferation occurred only when the T cells were in proximity to tumor cells. To do so, we isolated CD3^{+} T cells by negative selection magnetic bead sorting and assessed proliferation with anti-CD3 and anti-CD28 co-

stimulation. The isolated T cells still lacked proliferative capacity compared to WT mice, indicating that the T cells are indeed intrinsically dysfunctional (Fig 2c). Finally, we asked whether the AML-derived $CD8^+$ T cells were phenotypically terminally exhausted (TEx; $PD1^+$, $TIM3^+$, $TCF1^-$) or precursor/progenitor exhausted (TPEx; $PD1^+$, $TCF1^+$, $TIM3^-$), which have been shown to retain anti-tumor activity, predict clinical outcome, and expand with ICB[7, 9, 38-41]. Flow cytometric analysis of $PD1^+$ $CD8^+$ T cells derived from AML mice were primarily consistent with a TEx phenotype in contrast to WT mice, which were primarily TPEx (Fig 2d,e). Thus, the AML mice have an immunosuppressive microenvironment which drives $CD8^+$ and $CD4^+$ T cell exhaustion.

Ex vivo treatment of splenocytes from AML mice with BETi rescues T cell dysfunction

To identify rationally-derived combination treatment strategies which target tumor-intrinsic and extrinsic factors, we performed high-capacity drug screening as previously described[42] on tumor cells cultured from the AML mice. Interestingly, we found that three of the top six most efficacious small molecule inhibitors (SMIs) targeted BET proteins (JQ1, OTX-015, CPI-0610) (Fig 3a). Given previous works by Kagoya *et al.*, Zhu *et al.*, and Hogg *et al*. which established the role for BETi in maintaining stemness of $CD8^+$ T cells via inhibition of TCR-activated transcription factor BATF[35] and that BETi reduce immunosuppressive ligand PD-L1[33, 34], we asked whether BETi + anti-PD1 could impact the exhausted phenotype found in T cells from our AML mice. To test whether BETi could rescue T cell dysfunction and rescue ICB therapy resistance, we performed proliferation assays as previously described with whole splenocytes and anti-CD3 stimulation but also in the presence of 60nM BETi JQ1, 120nM JQ1, 60nM JQ1 + 10ug/mL anti-PD1, 120nM JQ1 + anti-PD1, or anti-PD1 alone. As expected, treatment with anti-PD1 alone had no effect on proliferation, as the T cells were shown to be primarily terminally exhausted (Fig 2d-g). However, treatment with JQ1 at 60nM, and more so with 120nM, significantly increased proliferation of AML-derived $CD8^+$ T cells, whereas WT T cells were unaffected. Moreover, the combination of 120nM JQ1 and anti-PD1 had the largest effect, with a median three-fold increase in $CD8^+$ T cell proliferation compared to anti-CD3 stimulation alone (Fig 3b, c). The benefit of adding BETi with anti-PD1 was also observed in $CD4^+$ T cells, but was more variable between individual mice, with some mice only marginally benefitting from combined treatment while others were dramatically enhanced (Fig S2a). We then assessed the efficacy of combining BETi + aPD1 in five primary AML patient samples with an array of mutational backgrounds. We found that all samples had T cell dysfunction and that 2/5 samples were rescuable with BETi or BETi + aPD1 (Fig S2b). We next asked what phenotype characterized these newly

proliferating $CD8^+$ T cells in the AML mice and found that they expressed high levels of TCF1 and low levels of TIM3, indicating that BETi mechanistically act by increasing TPEx:TEx ratios (Fig 3d-f).

In vivo-treated AML mice have reduced tumor burden and increased T cell TPEx gene program expression

We next sought to determine the *in vivo* efficacy of BETi in combination with anti-PD1 and whether they modulate the tumor microenvironment. We treated AML or WT mice with RIgG (200ug/injection), JQ1 (50mg/kg), anti-PD1(200ug/injection), or combined JQ1 and anti-PD1 (50mg/kg and 200ug/injection, respectively) for 14 days and measured white blood cell (WBC) count in blood pre-treatment, mid-treatment, and at endpoint and characterized the tumor microenvironment by flow cytometry (Fig 4a). Analysis of WBC counts over time found that only the combination of JQ1 + anti-PD1 significantly reduced tumor burden and, as expected from the *ex vivo* proliferation assays, anti-PD1 alone had no effect (Fig 4b). Characterization of the tumor microenvironment showed no significant changes to the frequency of regulatory T cells, MDSCs, or splenic $CD3^+$ T cells (Fig S3a,b, 4c). However, we observed a significant increase in $CD8^+$ T cells in the bone marrow in the JQ1 + anti-PD1 treatment mice, suggesting that this combination treatment is having a greater impact on $CD8^+$ T cells specifically and not on other immunosuppressive cell types (Fig 4d). Finally, evaluation of RNA-transcripts in isolated $CD8^+$ T cells derived from JQ1 treated or vehicle treated AML mice identified significantly increased expression of TPEx genes such as *TCF7*, *SLAMF6*, and *CXCR5* (Fig 4e). Together, these results highlight the potential of combining BETi and anti-PD1 to treat immunosuppressed T cells in AML, particularly in ICB-refractory cases.

Discussion

Immune checkpoint blockade in hematological malignancies

ICB therapy in the blood cancer setting is relatively new and although dozens of clinical trials are ongoing and actively recruiting [43], no large scale study has been completed evaluating the efficacy of anti-PD1 therapies in AML. Our lab previously described the functional immune microenvironment of 50 newly-diagnosed AML patient bone marrow samples[43] and found that only 41% of samples showed $CD8^+$ T cell proliferation comparable to healthy donor. Further, we found that the AML patient samples with the most profound immunosuppression (37%) had severely dysfunctional T cells with significantly decreased effector cytokine production such as IFN-γ, IL-2, and TNF-α, and increased expression of inhibitory checkpoint markers such as

CTLA-4. Of these non-proliferator AML samples, 6 of 18 samples were not rescued with ICB treatment *in vitro*, as defined by lack of proliferation and reduced production of effector molecules. Combination treatment regimens that potentially synergize and rescue terminally exhausted T cells may be the key to greater success with ICB therapy clinically. Smaller clinical trials have evaluated the efficacy of anti-PD1 + hypomethylating agents (HMA) but only a small subset, approximately 33%, responded to therapy[44], which is consistent with our *ex vivo* findings[43]. Phenotypic profiling of these responsive patients before and after anti-PD1 +/- HMA identified pre-therapy bone marrow and peripheral blood $CD3^+$ and $CD8^+$ levels as predictive of response. In addition, we previously described the synergistic combination of combining MEKi and anti-PD1[36]. We found that MEKi acted directly on both tumor cells and immune cells globally by reducing PD-L1 expression on patient samples and, at low doses, restored some proliferative function of AML-derived T cells. Thus, it is clear that treatment strategies that target both tumor-intrinsic factors as well as T cell suppression will be more effective. Here, we show the potential for BETi therapy to directly reprogram exhausted $CD8^+$ T cells to a more stem-like, $TCF1^-$expressing subtype which expands and proliferates in response to ICB in AML and identify a novel model which recapitulated cancer-driven immune exhaustion/PD-1 refractoriness.

Epigenetic regulation of T cell exhaustion

T cell exhaustion is driven by chronic antigen exposure and is accompanied by vast changes in the epigenetic landscape[13, 14, 45-47]. This T cell state is identifiable by three main traits: 1) increased expression of inhibitory receptors such as PD1, LAG3, TIGIT, and CTLA-4, 2) decreased secretion of effector cytokines such as IL-2, IFN-γ, TNF-α and 3) loss of proliferative capacity[14, 48-51]. These epigenetic changes are largely driven by a pool of coordinating TCR-responsive transcription factors, such as BATF, IRF4, TOX, and NFAT[6, 49-51], chromatin remodeling complexes such as EZH2, and other polycomb repressive complex 2 proteins[52-55]. Generation of TPEx cells rely on the de-repression of many critical pro-memory transcription factors such as TCF1, FOX01, and others as a consequence of targeted DNA methylation deposition acquired during early effector differentiation. Interestingly, the pro-exhaustion transcription factor TOX was found to also directly modulate histone acetylation via direct binding to histone acetyltransferase KAT7[14, 45, 56]. This critical role for epigenetic regulation of T cell exhaustion has garnered much interest in investigating the potential of several epigenetic targeting SMI, whose original design was directed towards targeting tumor-intrinsic epigenetic dysregulation[12]. Very recently, Milner *et al.* showed that BRD4 regulates T cell differentiation by promoting super-enhancer

activity at regions regulating key pro-exhaustion/differentiation genes such as *Id2*, *Cx3cr1*, and *Runx1*[57]. Using our unique mouse model of AML, we find that BET inhibition in combination with ICB therapy can lead to a shift from predominantly non-responsive T cells with a TEx phenotype to TPEx and the production of functional $CD8^+$ T cells. These results form the basis for further study of such combination therapies in AML. Further studies will focus on understanding the heterogeneity in AML patient responses to BETi + aPD1.

Methods

AML murine model

Mice expressing FLT3-ITD under the endogenous FLT3 promotor (strain B6.129-Flt3tm1Dgg/J, The Jackson Laboratory stock no. 011112) were crossed to mice with the Tet2 gene flanked by LoxP sites (strain B6;129S-Tet2tm1.1Iaai/J, The Jackson Laboratory stock no. 017573). The FLT3-ITD/Tet2 flox mice were then crossed to mice expressing CRE recombinase controlled by the LysM promotor (strain B6.129P2-Lyz2tm1(cre)Ifo/J, The Jackson Laboratory stock no. 004781). All breeding animals were purchased from The Jackson Laboratory. All mice used in these experiments were bred as heterozygous for FLT3-ITD, TET2, and LysCre. All mouse experiments were performed in accordance with Institutional Animal Care and Use Committee protocol IP00000907.

Flow Cytometry Staining

Bone marrow, blood, or splenocytes were processed and subjected to red blood cell (RBC) lysis by ACK before counting via hemacytometer. Five million cells were resuspended in PBS and stained with Zombie Aqua viability dye (Biolegend, Cat# 423102) for 15 minutes at room temperature, covered from light. The cells were then washed with FACS buffer (PBS, 2% calf serum, 0.02% sodium azide) and resuspended in 25 µL 1:50 mouse FC block (TruStain FcX, BioLegend Cat# 101320), and left on ice for 5 minutes. 25 µL of a 2x cell surface staining antibody cocktail was added directly on top of the cells (final FC block 1:100, 1x Ab concentration) and stained on ice for 30 minutes. For intracellular staining, the cells were then washed with FACS buffer, permeabilized and stained for intracellular targets according to manufacturer's protocol (eBioscience FOXP3 Transcription Factor Staining Buffer Set, Cat# 00-5523-00), then resuspended in FACS buffer before analyzing on either a BD Fortessa or Cytek Aurora flow cytometer. Data was analyzed using FlowJo software.

Mouse Marker	Clone	Vendor
Tbet	4B10	Biolegend
LAG-3	C9B7W	Biolegend
TIM3	RMT3-23	Biolegend
CD44	IM7	Biolegend
CD62L	MEL-14	Biolegend
PD-L1	10F.9G2	Biolegend
CD11b	M1/70	Biolegend
CD8a	53-6.7	Biolegend
GR1	RB6-8C5	Biolegend
PD-1	29F.1A12	Biolegend
BATF	S39-1060	Biolegend
CD34	HM34	Biolegend
CD3e	400A2	Biolegend
TCF1	C63D9	Cell Signaling Technologies
CD4	GK1.5	Biolegend
FOXP3	FJK-16S	Biolegend

Human Marker	Clone	Vendor
CD19	HIB19	BioLegend
CD45	HI30	BioLegend
CD8	RPA-T8	BioLegend
CTLA4	BNI3	BioLegend
PDL1	29E.2A3	BioLegend
CD33	WM53	BioLegend
CD4	RPA-T4	BioLegend
PDL2	24F.10C12	BioLegend
CD56	HCD56	BioLegend
TIGIT	MBSA43	ThermoFisher
TIM3	7D3	BD
PD1	EH12.2H7	BioLegend
CD3	HIT3a	BioLegend

H&E Histology

Liver, spleen, and bone marrow snips were fixed and cut into paraffin blocks for H&E staining. The slides were then scanned using an Aperio AT2 scanner and analyzed with ImageScope.

Long-term culture of AML mice-derived bone marrow cells and Inhibitor Library Screen

Bone marrow aspirates from three AML mice were combined, isolated, and cultured in RPMI containing 20% fetal bovine serum (FBS), streptomycin/penicillin, 50 µM 2-mercaptoethanol (RPMI-20), and supplemented with murine SCF (10 ng/ml) and IL-3 (10 ng/ml) (Peprotech or BioLegend). The cells were serially passaged for ~1 month. Inhibitor library screening to evaluate drug sensitivity was performed as previously described[42]. Briefly, AML mice-derived tumor cells were counted and seeded into four 384 well plates at a concentration of

2000 cells/well. The cells were then subjected to titrations of 188 unique small-molecule inhibitors in culture for 72 hours. MTS reagent (CellTiter96 AQueous One; Promega) was added and the optical density was read at 490 nm to assess viability.

Mouse ex vivo proliferation assays

96-well round-bottom plates were coated in either 2.5 µg/mL anti-CD3 (Biolegend, clone 145-2C11,Cat# 100359) or HIgG (Biolegend, clone HTK888, Cat#400959), at 4° C overnight, then washed with PBS. Splenocytes were harvested from AML or WT mice and stained with 2 µM CFSE (Life Technologies, Thermo Fisher) at $5x10^{6}$/mL at 37° C in the dark. After 15 minutes, the CFSE was quenched with 10 mL calf serum and washed with PBS. Cells were then plated at $5x10^{5}$/well in RPMI with 10% FBS with BME supplementation and penicillin/streptomycin (RPMI-10). After a 72-hour incubation at 37° C the cells were stained for flow cytometric analysis and analyzed as previously described. Anti-PD1 (Clone RMP1-14) and RIgG (2A3) were purchased from BioXCell. JQ1 was purchased from Cayman Chemical (#11187).

Human *ex vivo* proliferation assays

Bone marrow aspirates and peripheral blood samples were separated by Ficoll density gradient centrifugation. All experiments were performed using freshly isolated cells. Cells were labeled with CellTrace Violet (CTV, ThermoFisher) and cultured in 96-well plates coated with 1µg/ml anti-CD3 (Clone: UCHT1) or control mIgG (Clone: MOPC-21). Groups of wells were then treated with either 10µg/ml control mIgG, 10µg/ml anti-PD-1 (EH12.2H7), 60nM JQ1, or 60nM JQ1 + 10µg/ml anti-PD-1. After 5 days, cells were stained with antibodies specific to CD45 (HI30), CD3 (HIT3a), CD4 (RPA-T4), CD8 (RPA-T8), CD33 (WM53), CD38 (HIT2), PD-L1 (M1H1, Becton Dickinson), PD-L2 (24F.10C12), PD-1 (MIH4, BD), TIM3 (7D3, BD) and CTLA-4 (BNI3, BD). Viability was determined by Zombie Aqua staining and doublets were gated out of analysis by FSC-A vs FSC-H. Flow cytometry data was acquired on a BD LSRFortessa or Cytek Aurora and analyzed using FlowJo v10 software.

BETi + anti-PD1 treatment in vivo

Age range of AML mice used in in vivo experiments was 25 to 54 weeks. WT and AML mice were given seven doses of 200 µg RIgG, 50 mg/kg JQ1, 50 mg/kg JQ1 + 200 µg anti-PD1, or 200 µg anti-PD1 via i.p injection over two weeks (3 times per week, harvesting 1 day after 7th/final injection). Drug solutions were prepared in a solvent of 10% cyclodextrin in PBS from a stock solution of JQ1 (50 mg/mL) in DMSO, followed by

sonication/heat bath to dissolve the JQ1. Assessment of tumor burden in the blood, as determined by WBC measurements from Hemavet (950FS, Drew Scientific), was monitored weekly pre-, mid-, and post-treatment. At endpoint, single cell suspensions of bone marrow, blood, and spleen tissues were stained for flow staining as previously described.

Evaluation of CD8$^+$ T cell transcripts via Nanostring

AML mice were given 7 doses of vehicle, n = 5, (10% cyclodextrin) or 50 mg/kg JQ1, n = 5, via i.p injection over two weeks (3 times per week, harvesting 1 day after 7th/final injection) as previously. CD8$^+$ T cells were isolated by magnetic bead isolation (Biolegend #480136) and RNA extracted according to manufacture protocol (Zymogen #). Samples were hybridized and loaded onto the Nanostring Chipset according to manufacture instructions (Nanostring Panel NS_MM_CANCERIMM_C3400) and analyzed using the nSOLVER4.0 tool.

Author's Disclosure's

EFL has received research funding from Janssen, Celgene, Monojul, Ikena Oncology, Kronos Bio, Intellia Therapeutics and Amgen.

Author Contributions

K.A. Romine: Conceptualization, formal analysis, validation, investigation, visualization, methodology, writing-original draft, writing-review and editing. **H-J.C**: methodology, validation **Y.K**: Conceptualization, formal analysis, validation, investigation, writing-review and editing K.B: methodology **J.L.C**: methodology, writing-review and editing. **P.A.F**: methodology, writing-review, editing **M.T.N**: methodology **C.L**: methodology **J.S**: methodology **E.F.L**: Conceptualization, formal analysis, validation, investigation, writing-review and editing.

Acknowledgments

This work was funded by a grant NCI U54CA224019 and NCI U01 CA217862 to EFL. K.A.R was funded in part by a Program in Enhanced Research Training (PERT) T32 # 5T32GM071338-13. Flow Cytometry was performed at the OHSU Flow Cytometry Core Facility. C.L was funded by NLM 5 T15 LM 7088-28.

References

1. Dombret, H. and C. Gardin, *An update of current treatments for adult acute myeloid leukemia.* Blood, 2016. **127**(1): p. 53-61.
2. DiNardo, C.D. and J.E. Cortes, *Mutations in AML: prognostic and therapeutic implications.* Hematology Am Soc Hematol Educ Program, 2016. **2016**(1): p. 348-355.

3. Lagunas-Rangel, F.A., et al., *Acute Myeloid Leukemia-Genetic Alterations and Their Clinical Prognosis.* Int J Hematol Oncol Stem Cell Res, 2017. **11**(4): p. 328-339.
4. Specenier, P., *Nivolumab in melanoma.* Expert Rev Anticancer Ther, 2016. **16**(12): p. 1247-1261.
5. Carretero-Gonzalez, A., et al., *Analysis of response rate with ANTI PD1/PD-L1 monoclonal antibodies in advanced solid tumors: a meta-analysis of randomized clinical trials.* Oncotarget, 2018. **9**(9): p. 8706-8715.
6. Man, K., et al., *Transcription Factor IRF4 Promotes CD8(+) T Cell Exhaustion and Limits the Development of Memory-like T Cells during Chronic Infection.* Immunity, 2017. **47**(6): p. 1129-1141 e5.
7. Jadhav, R.R., et al., *Epigenetic signature of PD-1+ TCF1+ CD8 T cells that act as resource cells during chronic viral infection and respond to PD-1 blockade.* Proc Natl Acad Sci U S A, 2019. **116**(28): p. 14113-14118.
8. Wang, Y., et al., *The Transcription Factor TCF1 Preserves the Effector Function of Exhausted CD8 T Cells During Chronic Viral Infection.* Front Immunol, 2019. **10**: p. 169.
9. Siddiqui, I., et al., *Intratumoral Tcf1(+)PD-1(+)CD8(+) T Cells with Stem-like Properties Promote Tumor Control in Response to Vaccination and Checkpoint Blockade Immunotherapy.* Immunity, 2019. **50**(1): p. 195-211 e10.
10. Utzschneider, D.T., et al., *Early precursor T cells establish and propagate T cell exhaustion in chronic infection.* Nat Immunol, 2020. **21**(10): p. 1256-1266.
11. Scott-Browne, J.P., et al., *Dynamic Changes in Chromatin Accessibility Occur in CD8(+) T Cells Responding to Viral Infection.* Immunity, 2016. **45**(6): p. 1327-1340.
12. Blank, C.U., et al., *Defining 'T cell exhaustion'.* Nat Rev Immunol, 2019. **19**(11): p. 665-674.
13. Chen, Z., et al., *TCF-1-Centered Transcriptional Network Drives an Effector versus Exhausted CD8 T Cell-Fate Decision.* Immunity, 2019. **51**(5): p. 840-855 e5.
14. Khan, O., et al., *TOX transcriptionally and epigenetically programs CD8(+) T cell exhaustion.* Nature, 2019. **571**(7764): p. 211-218.
15. Szczepanski, M.J., et al., *Increased frequency and suppression by regulatory T cells in patients with acute myelogenous leukemia.* Clin Cancer Res, 2009. **15**(10): p. 3325-32.
16. Wang, L., et al., *VISTA is highly expressed on MDSCs and mediates an inhibition of T cell response in patients with AML.* Oncoimmunology, 2018. **7**(9): p. e1469594.
17. Lamble, A.J., et al., *Reversible suppression of T cell function in the bone marrow microenvironment of acute myeloid leukemia.* Proc Natl Acad Sci U S A, 2020. **117**(25): p. 14331-14341.
18. Williams, P., et al., *The distribution of T-cell subsets and the expression of immune checkpoint receptors and ligands in patients with newly diagnosed and relapsed acute myeloid leukemia.* Cancer, 2018.
19. Williams, P., et al., *The distribution of T-cell subsets and the expression of immune checkpoint receptors and ligands in patients with newly diagnosed and relapsed acute myeloid leukemia.* Cancer, 2019. **125**(9): p. 1470-1481.
20. Noviello, M., et al., *Bone marrow central memory and memory stem T-cell exhaustion in AML patients relapsing after HSCT.* Nat Commun, 2019. **10**(1): p. 1065.
21. Tan, J., et al., *Increased PD-1+Tim-3+ exhausted T cells in bone marrow may influence the clinical outcome of patients with AML.* Biomark Res, 2020. **8**: p. 6.
22. Filippakopoulos, P., et al., *Selective inhibition of BET bromodomains.* Nature, 2010. **468**(7327): p. 1067-73.
23. Yang, Z., et al., *Recruitment of P-TEFb for stimulation of transcriptional elongation by the bromodomain protein Brd4.* Mol Cell, 2005. **19**(4): p. 535-45.
24. Zhou, Q. and J.H. Yik, *The Yin and Yang of P-TEFb regulation: implications for human immunodeficiency virus gene expression and global control of cell growth and differentiation.* Microbiol Mol Biol Rev, 2006. **70**(3): p. 646-59.
25. Zuber, J., et al., *RNAi screen identifies Brd4 as a therapeutic target in acute myeloid leukaemia.* Nature, 2011. **478**(7370): p. 524-8.
26. Shi, J. and C.R. Vakoc, *The mechanisms behind the therapeutic activity of BET bromodomain inhibition.* Mol Cell, 2014. **54**(5): p. 728-36.
27. Itzen, F., et al., *Brd4 activates P-TEFb for RNA polymerase II CTD phosphorylation.* Nucleic Acids Res, 2014. **42**(12): p. 7577-90.
28. Valent, P. and J. Zuber, *BRD4: a BET(ter) target for the treatment of AML?* Cell Cycle, 2014. **13**(5): p. 689-90.
29. Coude, M.M., et al., *BET inhibitor OTX015 targets BRD2 and BRD4 and decreases c-MYC in acute leukemia cells.* Oncotarget, 2015. **6**(19): p. 17698-712.
30. Shi, X., et al., *JQ1: a novel potential therapeutic target.* Pharmazie, 2018. **73**(9): p. 491-493.

31. Fiskus, W., et al., *Superior efficacy of cotreatment with BET protein inhibitor and BCL2 or MCL1 inhibitor against AML blast progenitor cells.* Blood Cancer J, 2019. **9**(2): p. 4.
32. Berthon, C., et al., *Bromodomain inhibitor OTX015 in patients with acute leukaemia: a dose-escalation, phase 1 study.* Lancet Haematol, 2016. **3**(4): p. e186-95.
33. Hogg, S.J., et al., *BET-Bromodomain Inhibitors Engage the Host Immune System and Regulate Expression of the Immune Checkpoint Ligand PD-L1.* Cell Rep, 2017. **18**(9): p. 2162-2174.
34. Zhu, H., et al., *BET Bromodomain Inhibition Promotes Anti-tumor Immunity by Suppressing PD-L1 Expression.* Cell Rep, 2016. **16**(11): p. 2829-2837.
35. Kagoya, Y., et al., *BET bromodomain inhibition enhances T cell persistence and function in adoptive immunotherapy models.* J Clin Invest, 2016. **126**(9): p. 3479-94.
36. Moshofsky, K.B., et al., *Acute myeloid leukemia-induced T-cell suppression can be reversed by inhibition of the MAPK pathway.* Blood Adv, 2019. **3**(20): p. 3038-3051.
37. Shenghui, Z., et al., *Elevated frequencies of CD4(+) CD25(+) CD127lo regulatory T cells is associated to poor prognosis in patients with acute myeloid leukemia.* Int J Cancer, 2011. **129**(6): p. 1373-81.
38. Kallies, A., D. Zehn, and D.T. Utzschneider, *Precursor exhausted T cells: key to successful immunotherapy?* Nat Rev Immunol, 2019.
39. Miller, B.C., et al., *Subsets of exhausted CD8(+) T cells differentially mediate tumor control and respond to checkpoint blockade.* Nat Immunol, 2019. **20**(3): p. 326-336.
40. Sade-Feldman, M., et al., *Defining T Cell States Associated with Response to Checkpoint Immunotherapy in Melanoma.* Cell, 2018. **175**(4): p. 998-1013 e20.
41. Brummelman, J., et al., *High-dimensional single cell analysis identifies stem-like cytotoxic CD8(+) T cells infiltrating human tumors.* J Exp Med, 2018. **215**(10): p. 2520-2535.
42. Tyner, J.W., et al., *Functional genomic landscape of acute myeloid leukaemia.* Nature, 2018. **562**(7728): p. 526-531.
43. Lamble, A.J. and E.F. Lind, *Targeting the Immune Microenvironment in Acute Myeloid Leukemia: A Focus on T Cell Immunity.* Front Oncol, 2018. **8**: p. 213.
44. Daver, N., et al., *Efficacy, Safety, and Biomarkers of Response to Azacitidine and Nivolumab in Relapsed/Refractory Acute Myeloid Leukemia: A Nonrandomized, Open-Label, Phase II Study.* Cancer Discov, 2019. **9**(3): p. 370-383.
45. Yao, C., et al., *Single-cell RNA-seq reveals TOX as a key regulator of CD8(+) T cell persistence in chronic infection.* Nat Immunol, 2019. **20**(7): p. 890-901.
46. Seo, H., et al., *TOX and TOX2 transcription factors cooperate with NR4A transcription factors to impose CD8(+) T cell exhaustion.* Proc Natl Acad Sci U S A, 2019. **116**(25): p. 12410-12415.
47. Scott, A.C., et al., *TOX is a critical regulator of tumour-specific T cell differentiation.* Nature, 2019. **571**(7764): p. 270-274.
48. Wherry, E.J., et al., *Lineage relationship and protective immunity of memory CD8 T cell subsets.* Nat Immunol, 2003. **4**(3): p. 225-34.
49. Barber, D.L., et al., *Restoring function in exhausted CD8 T cells during chronic viral infection.* Nature, 2006. **439**(7077): p. 682-7.
50. Paley, M.A., et al., *Progenitor and terminal subsets of CD8+ T cells cooperate to contain chronic viral infection.* Science, 2012. **338**(6111): p. 1220-5.
51. Zajac, A.J., et al., *Viral immune evasion due to persistence of activated T cells without effector function.* J Exp Med, 1998. **188**(12): p. 2205-13.
52. Gray, S.M., et al., *Polycomb Repressive Complex 2-Mediated Chromatin Repression Guides Effector CD8(+) T Cell Terminal Differentiation and Loss of Multipotency.* Immunity, 2017. **46**(4): p. 596-608.
53. Pace, L., et al., *The epigenetic control of stemness in CD8(+) T cell fate commitment.* Science, 2018. **359**(6372): p. 177-186.
54. Ladle, B.H., et al., *De novo DNA methylation by DNA methyltransferase 3a controls early effector CD8+ T-cell fate decisions following activation.* Proc Natl Acad Sci U S A, 2016. **113**(38): p. 10631-6.
55. Youngblood, B., et al., *Effector CD8 T cells dedifferentiate into long-lived memory cells.* Nature, 2017. **552**(7685): p. 404-409.
56. Page, N., et al., *Expression of the DNA-Binding Factor TOX Promotes the Encephalitogenic Potential of Microbe-Induced Autoreactive CD8(+) T Cells.* Immunity, 2018. **48**(5): p. 937-950 e8.

57. Milner, J.J., et al., *Bromodomain protein BRD4 directs and sustains CD8 T cell differentiation during infection.* J Exp Med, 2021. **218**(8).

Figure 1: Mouse Model Characterization

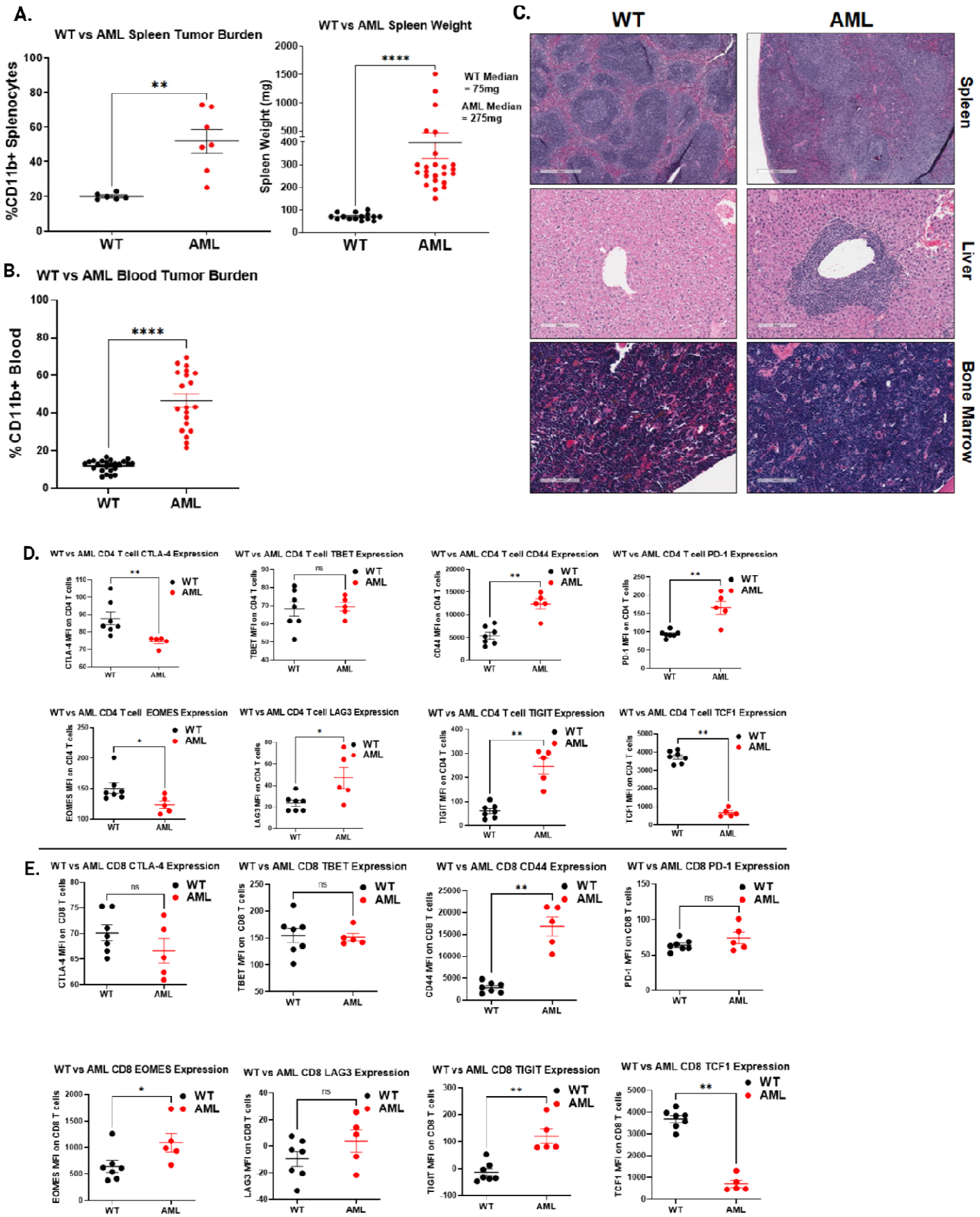

a.) Splenocytes isolated from *FLT3-ITD +/-, TET2 +/-, LysCre +/-* (AML, red) or C57BL/6 (WT, black) mice were isolated and stained as described for live CD11b+ cells and evaluated by flow cytometry. Significance determined by Mann-Whitney T-test.

b.) Spleens were isolated from 15 WT (black) and 24 AML (red) mice and weighed. Median weights for each group displayed on right side of plot. Significance determined by Mann-Whitney T-test.

c.) Blood isolated from 24 WT (black) and 20 AML (red) mice and stained as described for live CD11b+ cells and evaluated by flow cytometry. Significance determined by Mann-Whitney T-test.

d.) Representative H&E staining of WT and AML mice-derived spleen (Top row, 500 µm scale), liver (middle row, 200 µm scale), and bone marrow (bottom row, 100 µm scale).

e.) Briefly, splenocytes from untreated WT (black) and AML (red) mice were assessed for expression, via median fluorescence intensity, of markers of immune exhaustion on CD4 T cells (Live, CD11b-, CD3+, $CD4^+$). Top row (Left to right: CTLA-4, TBET, CD44, PD-1). Bottom Row (Left to right: EOMES, LAG3, TIGIT, TCF1). Significance determined by multiple Mann-Whitney T-tests. CD44, PD-1, LAG3 significantly increased in AML mice. CTLA-4, EOMES, and TCF1 significantly decreased in AML mice.

f.) Briefly, splenocytes from untreated WT (black) and AML (red) mice were assessed for expression, via median fluorescence intensity, of markers of immune exhaustion on $CD8^+$ T cells (Live, CD11b-, CD3+, $CD8^+$). Top row (Left to right: CTLA-4, TBET, CD44, PD-1). Bottom Row (Left to right: EOMES, LAG3, TIGIT, TCF1). Significance determined by multiple Mann-Whitney T-tests. CD44, EOMES, and TIGIT significantly increased in AML mice. TCF1 significantly decreased in AML mice.

Figure 2: AML mouse-derived CD8$^+$ T cells are intrinsically dysfunctional and unresponsive to TCR stimulation

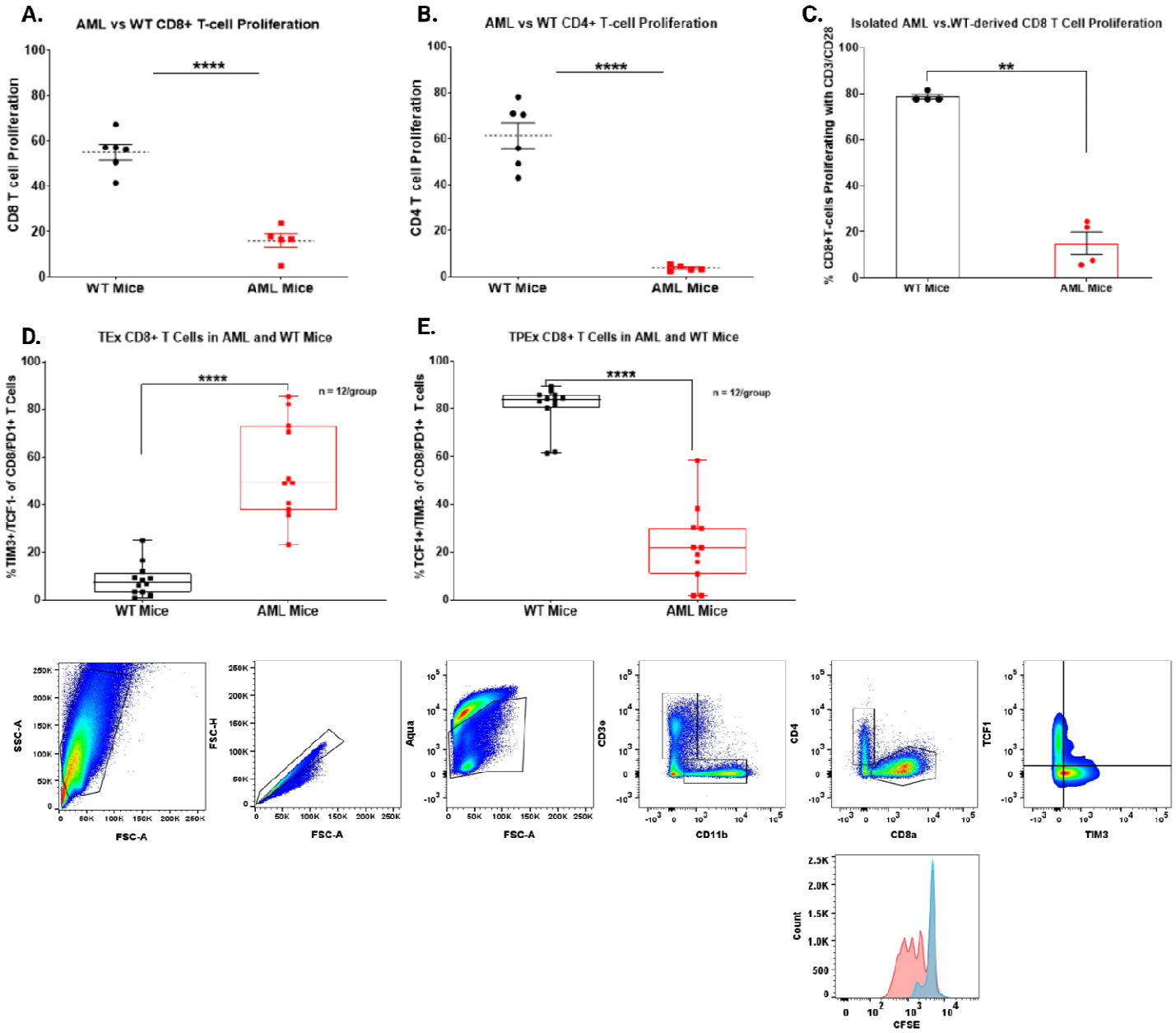

a, b.) WT (black) and AML (red) splenocytes were isolated, stained with proliferation dye (CFSE), and cultured for 72 hours with anti-CD3. Proliferation of a.) CD8$^+$ T cells and b.) CD4$^+$ T cells was then assessed by flow cytometry, staining with viability and markers to identify T cells. Proliferation displayed is percent CFSE diluted relative to unstimulated (HIgG) control for each cell type. Significance determined by Mann-Whitney T-tests.

c.) WT (black) and AML (red) T cells were isolated from splenocytes via CD3 negative isolation magnetic beads. The T cells were then stained with CFSE and plated for 72 hours with anti-CD3 and anti-CD28 stimulation. The cells were then harvested and assessed by flow cytometry. Significance determined by Mann-Whitney T-test.

d., e.) Splenocytes derived from WT (black) and AML (red) mice were stained for surface and intracellular markers of T cells exhaustion and evaluated by flow cytometry. d.) Terminally Exhausted CD8 T cells (TEx) are represented as %TIM3$^+$/TCF1$^-$ of the CD8$^+$/PD1$^+$ T cells. e.) Progenitor Exhausted CD8 T cells (TPEx)

are represented as %TCF1^{+}/TIM3^{-} of the CD8^{+}/PD1^{+} T cells. Significance determined by Mann-Whitney T-tests. Plots below are a representative example from an AML mouse demonstrating the gating scheme used to assess T cell phenotype and proliferation.

Figure 3: AML mice T cells are refractory to ICB therapy but partially rescued with BET inhibition *ex vivo*

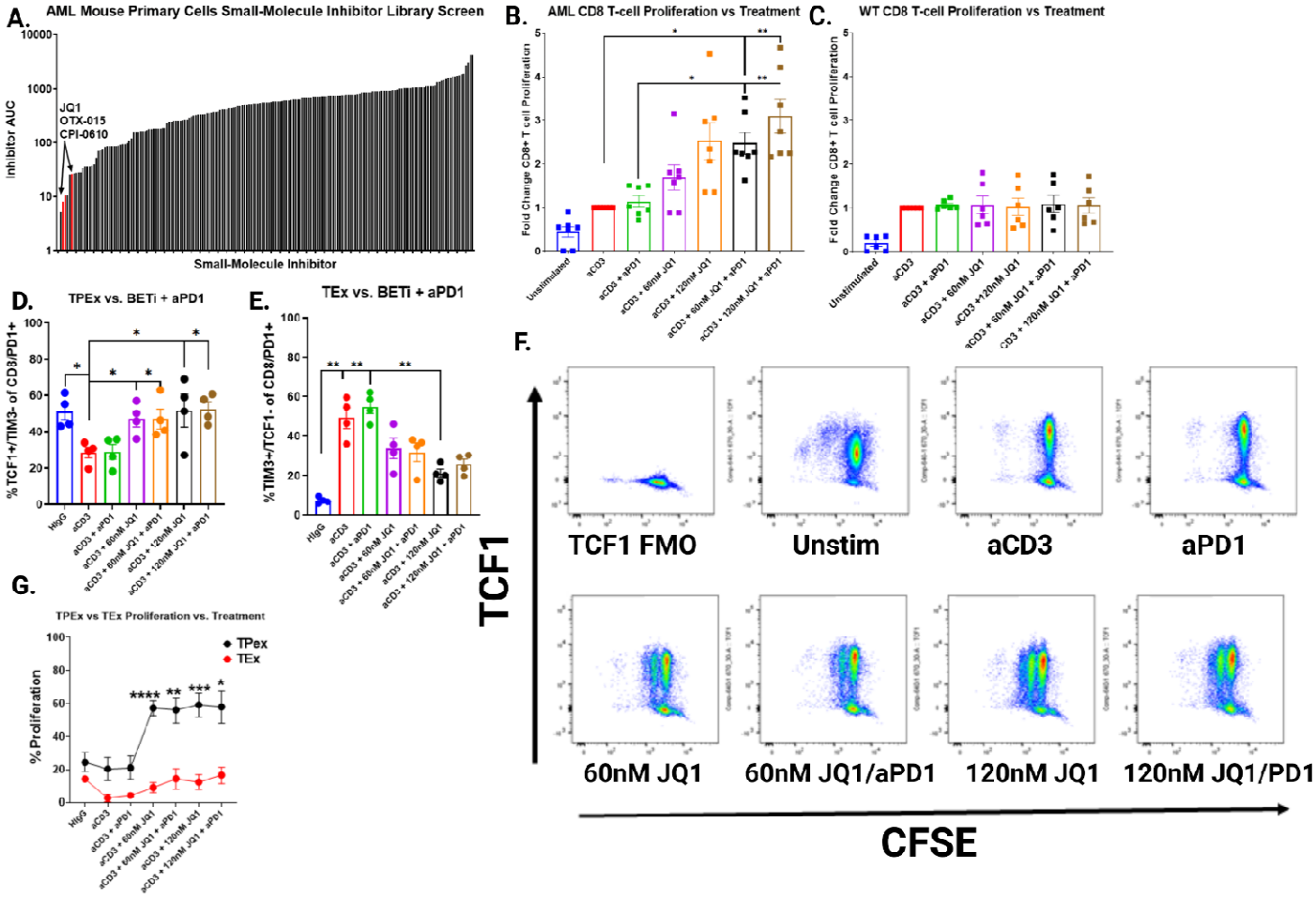

a.) AML cells passaged for ~ 1 month were subjected to an inhibitor library panel, as previously described[42]. Briefly, cells were counted and seeded into multiple 384 well plates containing titrations to 188 inhibitors, incubated for 72 hours, and viability assessed by MTS assay. Plot represents each Areas Under the Curve (AUC) for every inhibitor on the panel. BET inhibitors JQ1, OTX-015, and CPI-0610 are highlighted in red.

b., c.) Splenocytes were isolated from b.) 7 AML or c.) 6 WT mice, stained with CFSE, and cultured for 72 hours without TCR stimulation (HIgG), anti-CD3 alone, anti-CD3 with anti-PD1 alone, and titrations of anti-CD3 with JQ1 or anti-CD3 with both JQ1 and anti-PD1. Cells were then harvested and stained for assessment by flow cytometry. Plots represent the fold change in proliferation in CD8 T cells, as measured by percent CFSE diluted relative to anti-CD3 stimulated alone. Significance determined by Kruskal-Wallis multiple comparisons T-tests.

d., e.) Effect of BETi, aPD1, or BETi + aPD1 treatment on the percent of d.) TPEx $CD8^+$ T cells and e.) TEx $CD8^+$ T cells after culturing for 72 hours as previously in b-c. Significance determined by Kruskal-Wallis multiple comparisons T-tests.

f.) Splenocytes were isolated from 4 AML mice, stained with CFSE, and plated for 72 hours without TCR stimulation (HIgG), anti-CD3 alone, anti-CD3 with anti-PD1 alone, and titrations of anti-CD3 with JQ1 or anti-CD3 with both JQ1 and anti-PD1. Proliferation of specifically TPEx (black) and TEx (red) $CD8^+$ T cells in AML mice was assessed by flow cytometry. Significance determined by Kruskal-Wallis multiple

comparisons T-tests. Representative flow dot plot (right) shows CFSE (x-axis) vs TCF1 (y-axis) on $CD8^+$ T cells.

Figure 4: *in vivo* treatment with BETi and anti-PD1 synergizes in reducing tumor burden and enhances CD8 T cell activity

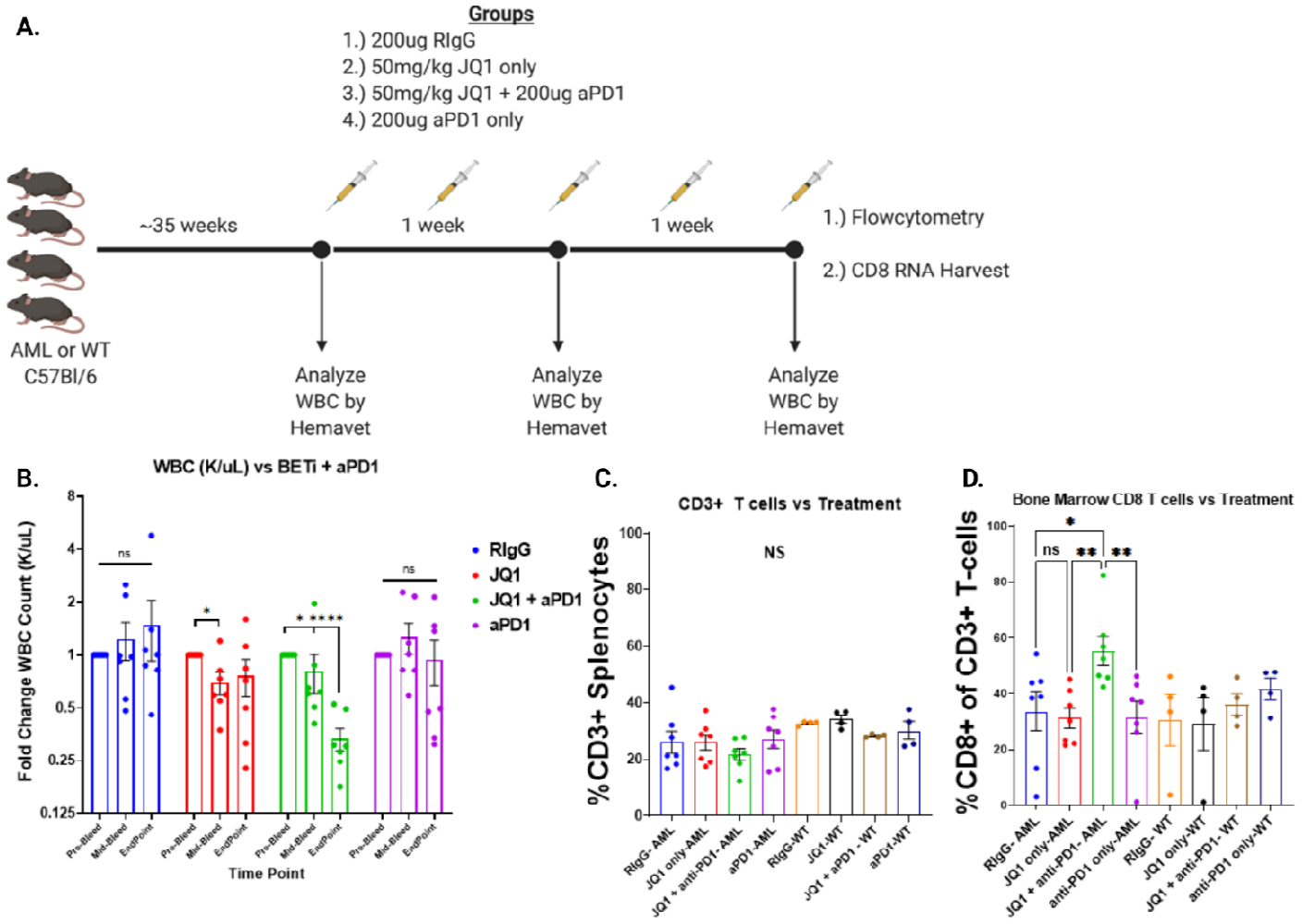

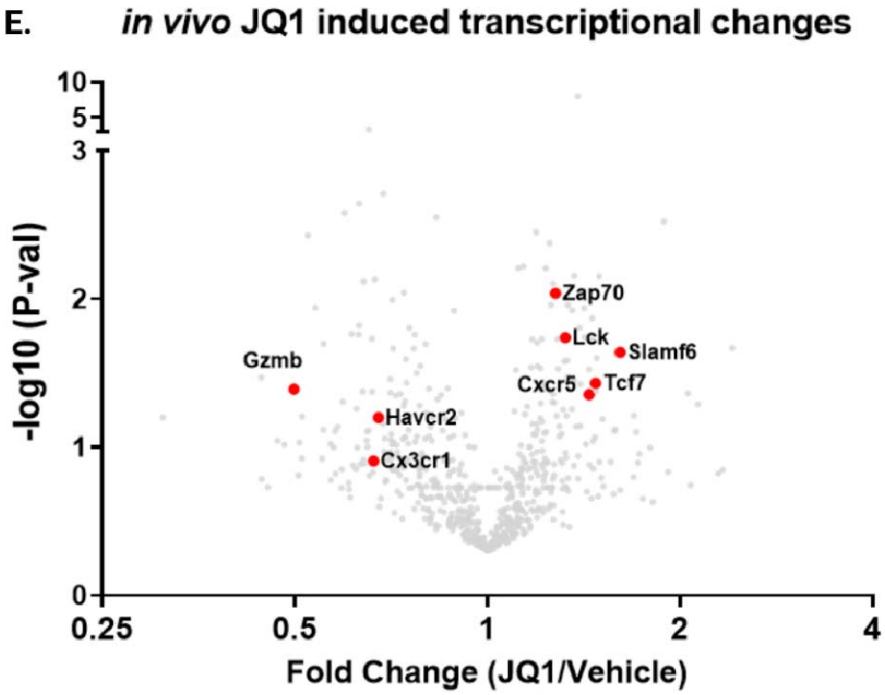

a.) Schematic detailing *in vivo* BETi + anti-PD1 treatment strategy and functional readouts of efficacy.

b.) Mice treated with RIgG, JQ1, JQ1 + anti-PD1, or anti-PD1 alone were bled periodically over a two-week period and white-blood cell count assessed by hemavet. Data displays fold change WBC (k/µL) normalized per mouse (ie mid-point = Mouse A day 7 WBC/Mouse A Day 0 WBC, etc.). Significance determined by one-way anova. X-axis indicates time point (Pre-Bleed = day 0, Mid-bleed = day 7, Endpoint = day 14). Y-axis indicates fold change WBC (k/µL).

c, d.) Bone marrow cells were isolated from treated AML and WT mice and assessed by flow cytometry. Graph denotes c.) %CD3+ T cells in the bone marrow vs treatment and d.) %$CD8^+$ T cells in the bone marrow as a percent of all T cells. Significance derived from combining two experimental replicates and determined by one-way anova.

e.) $CD8^+$ T cells were isolated from JQ1 treated and RIgG treated AML mice and RNA harvested and analyzed by nanostring. Volcano plot shows the fold change in normalized transcript levels of JQ1 treated mice vs RIgG treated AML mice vs. $-\log_{10}$ P-value as determined by multiple t-tests. Hits of interest highlighted in red. Dashed red line denotes significance threshold (0.05).

Supplemental Figures

Supplemental Figure 1: Treg, MDSC, and total T cell frequencies in AML and WT mice

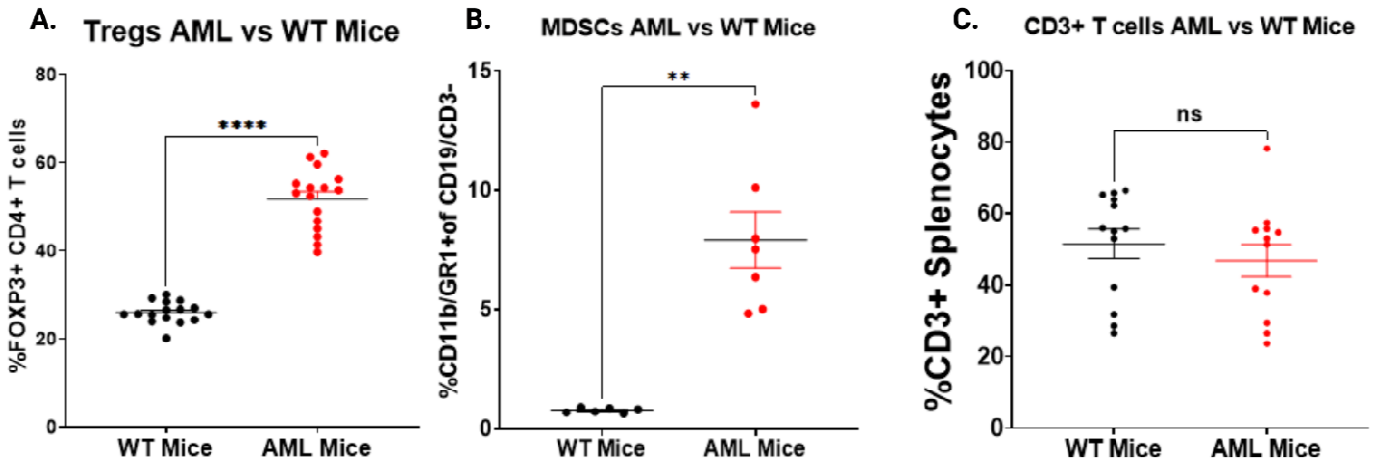

a-c.) Splenocytes isolated from *FLT3-ITD +/-, TET2 +/-, LysCre +/-* (AML, red) or C57BL/6 (WT, black) mice were isolated and stained as described for a.) Treg cells – $CD4^{+}$, FOXP3+, b.) MDSCs – CD11b+, GR1+, and c.) All T cells – CD3+, and evaluated by flow cytometry. Significances determined by Mann-Whitney T-tests.

Supplemental Figure 2: CD4^{+} T cell *ex vivo* proliferation vs BETi + aPD1

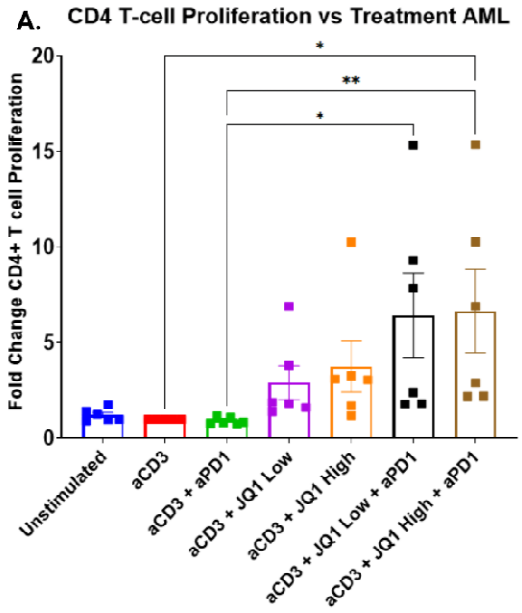

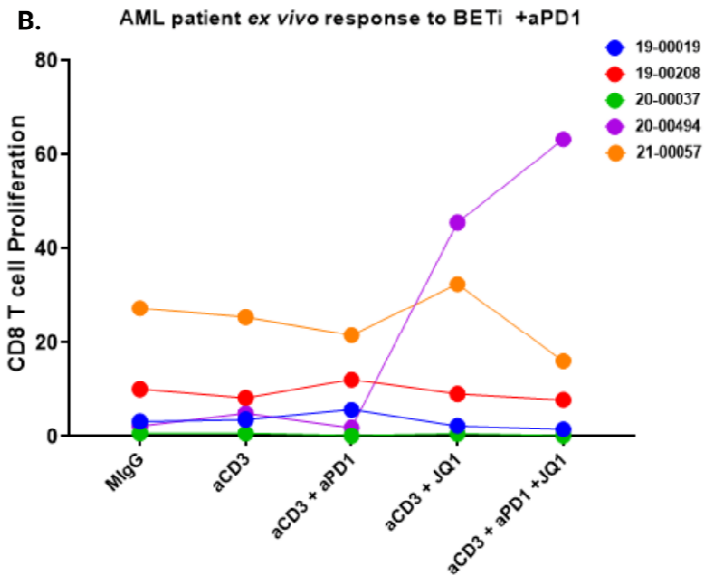

Pt ID	Mutations							JQ1 Responder?
19-00019	CEBPA	DNMT3A	GATA2	NRAS				NO
19-00208	FLT3-ITD							NO
20-00037	CEBPA	DNAH9	DOCK8	EGFR	EZH2	GATA2	NPM1	NO
20-00494	DNMT3A	IDH2	NT5CS2	RUNX1	ASXL1	BCOR		YES
21-00057	SMC1A	PTPN11	NPM1	DNMT3A	IDH1			YES

a.) Splenocytes were isolated from b.) 6 AML mice stained with CFSE, and cultured for 72 hours without TCR stimulation (HIgG), anti-CD3 alone, anti-CD3 with anti-PD1 alone, and titrations of anti-CD3 with JQ1 or anti-CD3 with both JQ1 and anti-PD1. Cells were then harvested and stained for assessment by flow cytometry. Plots represent the fold change in proliferation in CD4 T cells, as measured by percent CFSE diluted relative to anti-CD3 stimulated alone. Significance determined by Kruskal-Wallis multiple comparisons T-tests.

b.) Bone marrow aspirates derived from 6 AML patient samples were stained with cell trace violet and cultured for 5 days without TCR stimulation (RIgG), anti-CD3 alone, anti-CD3 with 120 nM JQ1, or anti-CD3 with 120 nM JQ1 and anti-PD1. Cells were then harvested and stained for assessment by flow cytometry. Plots represent raw CD8^{+} T cell proliferation for each patient sample. Below is the corresponding mutations for each patient.

Supplemental Figure 3: Treg and MDSCs vs *in vivo* BETi + anti-PD1 treatment

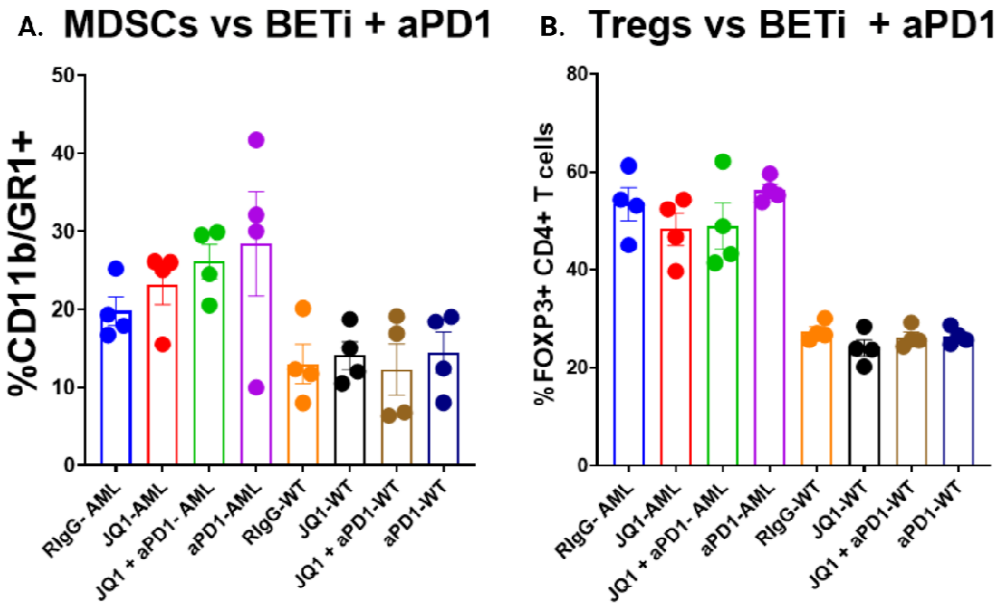

a., b.) Splenocytes derived from AML mice treated with RIgG, JQ1, JQ1 + aPD1, or anti-PD1 were assessed by flow cytometry to determine a.) %MDSCs (CD11b+GR1+) and b.) %Tregs ($CD4^{+}FOXP3+$). No significance was observed between treatments in AML or WT mice independently.